Korean J. Chem. Eng., 38(5), 1023-1031 (2021)
DOI: 10.1007/s11814-021-0749-9

pISSN: 0256-1115
eISSN: 1975-7220

Experimental and modeling studies for intensification of mercaptans extraction from LSRN using a microfluidic system

Mohammad Reza Mirani*, Alireza Fazlali*,†, and Masoud Rahimi**

*Department of Chemical Engineering, Faculty of Eng., Arak University, Arak, Iran
**CFD research center, Chemical Engineering Department, Razi University, Kermanshah, Iran
(*Received 21 October 2020 • Revised 18 January 2021 • Accepted 26 January 2021*)

Abstract−We investigated the performance of a T-type microchannel for mercaptan extraction from light straight-run naphtha (LSRN) with sodium hydroxide solution. The aim of this work is to introduce the microfluidic system as a potential tool for mercaptan extraction from light petroleum products. Modeling the extraction process of mercaptan from LSRN has not been carried out previously. In this regard, mercaptan extraction was modeled by response surface methodology (RSM) and artificial neural network (ANN) to analyze the effect of operating parameters on the mercaptan extraction process. The independent variables are considered as temperature, sodium hydroxide concentration, and the volume ratio of sodium hydroxide to LSRN. Two models were compared based on error analysis of the predicted data. Root mean square error, mean relative error, and determination coefficient for the neural network were 0.5650, 0.4341, and 0.9862, respectively. The values of these parameters for the RSM model were 0.6854, 0.7648, and 0.9798. The results showed that the prediction accuracy for both models is appropriate, but the precision of the neural network model is slightly higher than that of the RSM model. The genetic algorithm (GA) technique determined the optimal values of the independent variables with the aim of maximizing the extraction percentage. The mercaptan extraction percentage value of 85.08% was achieved at 303.15 K, the sodium hydroxide concentration of 20 wt%, and the volume ratio of sodium hydroxide to LSRN of 0.128. Furthermore, results showed a higher mercaptan extraction percentage of the microfluidic system compared to a conventional extractor at the same process condition.

Keywords: Microchannel, Mercaptan Extraction, Light Straight-run Naphtha, Genetic Algorithm, Optimization, RSM, ANN

INTRODUCTION

Mercaptans are organosulfur compounds composed of an alkyl or aryl group with a thiol group. They have a foul odor and can cause corrosion in pipelines, so demercaptanization processes are widely applied for many petroleum products [1]. There are various methods to remove mercaptans from petroleum products, but the major procedures are catalytic oxidation and extraction with alkaline solution [2-5]. In the catalytic oxidation method, light and heavy mercaptans are oxidized by air to form disulfides in the presence of alkaline solution and Merox catalyst. In this process, disulfides remain in the products, so total sulfur content does not decrease. This technology was licensed in 1958 by the UOP company for demercaptanization of liquid petroleum products [6]. The extraction procedure with an alkaline solution is extensively utilized for removing light mercaptans from liquid hydrocarbons [7]. In this method, in addition to the light mercaptans, carbonyl sulfides (COS) and carbon disulfides (CS_2) are extracted, too. Therefore, this method plays an important role in the sweetening process of liquid hydrocarbons. Mercaptan extraction depends on their solubility in alkaline solution. As the molecular weight of mercaptan increases, their solubility in alkaline solution decreases [2]. Mercaptan removal using extraction procedure is mostly used for sweetening light distillation cuts like light straight-run naphtha (LSRN) and liquefied petroleum gas (LPG). Temperature, alkaline solution concentration, and the volume ratio of alkaline solution to hydrocarbon are effective parameters in the mercaptan extraction process. Many researchers have studied the effect of process parameters on the mercaptan extraction from different hydrocarbons [8-12]. Afshar et al. [9] studied the effect of process parameters on mercaptan extraction from propane and butane with the alkaline solution in an extraction tower. They also reported the optimized values of operating parameters for LPG sweetening. Parvareh and Parvizi [13] studied the role of proper mixing for mercaptan extraction from kerosene with sodium hydroxide in a static mixer. They investigated the effect of mixer length and mixer element pitch at different flow rates of kerosene on the mercaptan removal. In a comprehensive investigation, Akopyan et al. [14] examined the mercaptan extraction from light hydrocarbon fractions with aqueous ammonia and alkaline solution in a sealed glass equipped with a magnetic stirrer. They studied the effect of solvent concentration, temperature, two-phase ratio, extraction durations, the rotation speed of stirrer, and initial content of mercaptan on the extraction efficiency. Furthermore, the influence of process parameters on the extraction efficiency of different mercaptan compounds, such as methyl thiol, ethyl thiol and propyl thiol, was examined. The results demonstrated that at the same extraction conditions, methyl thiol had the highest extraction efficiency, and as the molecular weight of mercaptans increases, the extraction effi-

†To whom correspondence should be addressed.
E-mail: a-fazlali@araku.ac.ir

ciency decreases.

In the mercaptan extraction process, like other extraction processes, access to a high contact surface between two phases is of great importance. Microchannels as an alternative to conventional extractors can improve mass transfer between two phases in different processes. [15,16]. In microfluidic systems, an increase in feed flow can be achieved with parallel cascade arrangements of microchannels [17]. Many researchers have investigated the performance of microchannels for various liquid-liquid extraction processes [18-21]. Microchannels provide a high specific interfacial area of two phases and decrease the diffusion distance [22,23]. The mass transfer rate in various shapes of microchannels is higher compared to the conventional extractors [18,24]. Darekar et al. [24] performed liquid-liquid extraction experiments in two types of microchannels using Zinc-D2EHPA system. The overall volumetric mass transfer coefficients of the microchannels were higher than those of a hollow fiber contactor.

In the last decade, the optimization of various extraction processes has been performed by many researchers [25,26]. Design of experiments and process modeling are common methods to examine the effect of individual parameters on the process's efficiency and find the optimal values of parameters. Response surface methodology (RSM) is an efficient technique for process modeling [27]. One of its advantages is that fewer tests are required to predict a reliable response. RSM also generates a polynomial regression model for predicting output response as well as analyzing individual parameters. Artificial neural network (ANN), another mathematical method for process modeling [28], was developed based on the behavior of the biological neural system. ANN has shown great accuracy in solving complex non-linear functions. It is considered a technique with higher accuracy and flexibility for modeling complex non-linear systems compared to RSM because it can learn based on observations and draw conclusions through generalization [29,30].

In the present study, a microfluidic system was employed to intensify the mercaptan extraction from LSRN with sodium hydroxide solution. To the best of our knowledge, mercaptan extraction from LSRN using microfluidic systems has not been investigated by other researchers. A T-type microchannel was utilized and the effect of independent parameters on the mercaptan extraction percentage was studied. The most important advantage of this study is to introduce the microfluidic system as a potential tool for demercaptanization of light petroleum products. To ensure the high performance of the microfluidic system, a comparison was performed between the mercaptan extraction percentage of the microfluidic system and that of a conventional extractor. Proposing trustworthy prediction models is required for determining the effective process parameters. Although there are many cases of modeling study in the field of mass transfer, few search studies have been dedicated to modeling liquid-liquid extraction in microfluidic systems. In this regard, RSM and ANN models were used to assess the effect of process parameters on the mercaptan extraction in different conditions of process parameters. There is not any literature reporting the performance comparison of ANN and RSM for mercaptan extraction from LSRN. The input parameters of the two models were temperature, sodium hydroxide concentration, and the vol-

Table 1. LSRN properties

Properties	Unit	Test method	Result
Specific gravity at 288.71 K	-	ASTM D-4052	0.67
Initial boiling point	K	ASTM D-86	316.15
End boiling point	K	ASTM D-86	388.15
Aromatic	vol%	ASTM D-6839	3.30
Paraffin	vol%	ASTM D-6839	89
Naphten	vol%	ASTM D-6839	3.20
Olefin	vol%	ASTM D-6839	4.50
Reid vapor pressure	kPa	ASTM D-323	68
Mercaptan content	ppmw	UOP-163	210
H_2S	ppmw	UOP-163	2

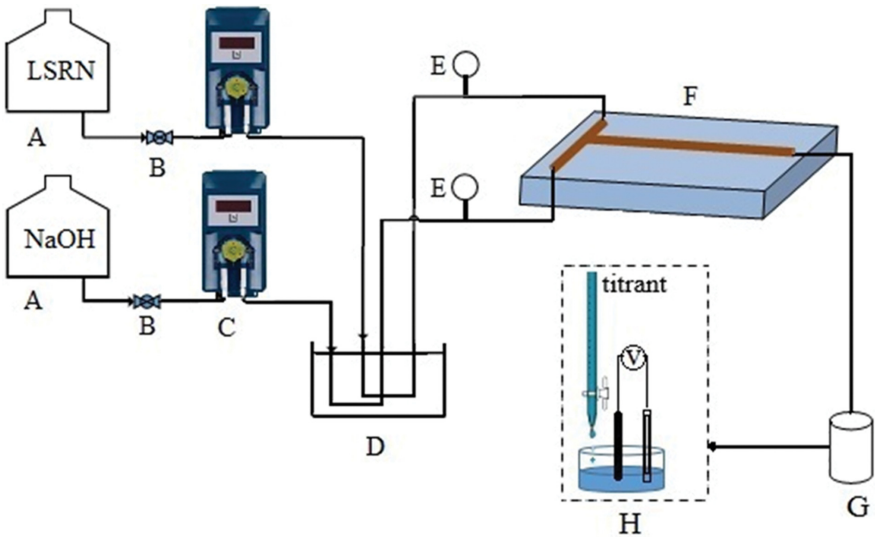

Fig. 1. Schematic diagram of the experimental setup: (A) liquid tank, (B) needle valve, (C) dosing (peristaltic) pump, (D) water bath, (E) temperature indicator, (F) microchannel, (G) sample, and (H) potentiometric titration.

ume ratio of sodium hydroxide to LSRN. Moreover, the GA technique was applied to obtain the optimal value of input parameters with the aim of maximizing the extraction percentage.

EXPERIMENTAL

1. Materials

Sodium hydroxide with a purity of more than 99% was provided from the Merck company. Deionized water was applied for preparing different concentrations of sodium hydroxide solution. Light straight-run naphtha (LSRN) was supplied from Kermanshah oil refinery company (KORC), which is located in the west of Iran. LSRN was exactly sampled after the prewash vessel of the LSRN sweetening unit. Table 1 illustrates the properties of employed LSRN.

2. Experimental Procedures

Mercaptans were extracted from the LSRN by sodium hydroxide solution in a microfluidic system. A schematic diagram of the employed experimental apparatus in this work is shown in Fig. 1. A glass T-shaped microchannel with a mixing length of 0.45 m and an internal diameter of 850×10^{-6} m was applied to perform experiments. Two dosing peristaltic pumps (from Lead Fluid Technology Company, China) were used for injecting two phases into the microchannel. The experiments were performed at the 303.15-313.15 K. LSRN as the organic phase and sodium hydroxide solution as the aqueous phase was pumped from two pipes, which were immersed in a bath of water to adjust the temperature of the two phases. The volumetric flow rate of sodium hydroxide solution was varied from 3.33×10^{-8}-10×10^{-8} (m^3/s) by the dosing peristaltic pump, while the LSRN flow rate was kept at 6.67×10^{-7} (m^3/s), so the volume ratio of sodium hydroxide solution to LSRN varied between 0.05 and 0.15.

After the extraction process was complete, the mercaptan concentration of sweetened LSRN was determined by UOP 163-10 standard test method. In this analysis method, hydrogen sulfide and mercaptan content of petroleum products are calculated based on a potentiometric titration with alcoholic silver nitrate [31]. To ensure the accuracy of the measurement, all of the experiments were repeated three times.

THEORETICAL CONSIDERATIONS

Mercaptans are organosulfur compounds that have the general formula of R-S-H [32]. In this sweetening process, light mercaptans are extracted from the LSRN by sodium hydroxide solution. The mechanism of mercaptan extraction with sodium hydroxide can be described by the following reaction [32].

$$RSH + NaOH \leftrightarrow RSNa + H_2O \quad (1)$$

Sodium mercaptide and water are the products of mercaptan reaction with sodium hydroxide. Additionally, the overall extraction constant is expressed by the following equation [2]:

$$K_E = \frac{RS^-_{aq} + RSH_{aq}}{RSH_{org}} \quad (2)$$

where $(RS^-)_{aq}$ and $(RSH)_{aq}$ are the concentration of ionized and neutralized mercaptan in the aqueous phase. The degree of completeness of mercaptans extraction depends on the mercaptan solubility in the alkaline solution, so temperature and sodium hydroxide concentration can affect K_E and subsequently the mercaptan extraction [14]. Furthermore, mercaptan extraction depends on the molecular weight and structure of the mercaptan. Mercaptans with low molecular weight are almost completely soluble in alkaline solution and as the molecular weight of mercaptan increases, solubility decreases. Thus, mercaptans with longer carbon chains have less solubility in alkaline solution [2].

In this study, mercaptan extraction was intensified by the applied microfluidic system due to the high specific interfacial area of two phases in these devices. To evaluate the microchannel performance, the extraction percentage was applied as the following equation [33]:

$$\%\,E = \frac{M_{org,\,in} - M_{org,\,out}}{M_{org,\,in}} \times 100 \quad (3)$$

where $M_{org,\,in}$ and $M_{org,\,out}$ represent mercaptan concentration of organic phase at inlet and outlet of the microfluidic system, respectively.

MODELING STUDY

1. Response Surface Methodology (RSM)

A five-level three-factorial CCD (central composite design) was applied for the modeling study [34]. Design-Expert (Stat-Ease, trial version) software was utilized for experimental design. The regression model for the mercaptan extraction process is demonstrated as the following equation:

$$Y = \beta_0 + \sum_{j=1}^{m}\beta_j X_j + \sum_{j=1}^{m}\beta_{jj} X_j^2 + \sum_{i<j}^{m}\sum_{j=2}^{m}\beta_{ij} X_i X_j + \ldots + e_i \quad (4)$$

where Y shows the predicted response, X_j and X_i are the independent variables, and m is the number of variables. β_0, β_j, β_{jj}, and β_{ij} are constant, linear, quadratic, and interaction coefficients, respectively. Additionally, e_i depicts the error.

Temperature, sodium hydroxide concentration, and the volume ratio of sodium hydroxide to LRSG were applied as input variables with five levels. Table 2 shows the range of variables. Also, temperature, sodium hydroxide concentration, and the volume ratio

Table 2. Input variables and applied levels in experiments

Factor	Independent variables	Unit	Coded values				
			−2	−1	0	1	2
X_1	Temperature	K	303.15	305.65	308.15	310.65	313.15
X_2	Sodium hydroxide concentration	wt%	10	12.5	15	17.5	20
X_3	Volume ratio of NaOH to LRSG	-	0.05	0.075	0.10	0.125	0.15

of two phases are indicated with X_1, X_2, and X_3, respectively.

2. Artificial Neural Network (ANN)

ANN is a useful tool for artificial intelligence that is extensively utilized for modeling unknown or semi-unknown processes [35]. AAN has been widely used in the modeling of nonlinear multivariate processes. In this study, a multi-layer perceptron ANN-based feedforward was applied for modeling of the mercaptan extraction process. One hidden layer was employed for the proposed neural network. Levenberg-Marquardt backpropagation algorithm was utilized for network training [36]. In this algorithm network, biases and weights are initialized randomly, and the network was developed by adjusting weights and biases. The process of network training was started with one neuron, and the number of hidden neurons was increased to reach an acceptable level of the model deviation. Logarithmic sigmoid (Logsig) and hyperbolic tangent sigmoid (Tansig) were used as transfer functions of the hidden layer, and Linear (Purelin) was utilized as output layer transfer function. The general forms of these transfer functions are expressed through the following equations:

$$\text{Logsig:} \quad F_t(x) = \frac{1}{1+e^{-x}} \tag{5}$$

$$\text{Tansig:} \quad F_t(x) = \frac{2}{1+e^{-2x}} - 1 \tag{6}$$

$$\text{Purelin:} \quad F_t(x) = x \tag{7}$$

The network output can be formulated as follows [37]:

$$y = F_{out}\left\{\sum_{j=1}^{n} W_{zj}\left[F_H\left(\sum_{i=1}^{m} W_{ji}X_i + b_j\right)\right] + b_z\right\} \tag{8}$$

where y, X, n, and m are the predicted response of the ANN model, input values, number of neurons, and number of input variables, respectively. F_{out} and F_H are transfer functions of the output and hidden layers, respectively. Furthermore, all input data were normalized to avoid any computational problem in network training. Input data were normalized between −1 and 1 as the following equation:

$$X_{norm} = 2\left(\frac{x - x_{min}}{x_{max} - x_{min}}\right) - 1 \tag{9}$$

where x_{min}, x_{max}, x, and X_{norm} are minimum value, maximum value, actual value, and normalized value, respectively.

Generally, in this work, the optimal neural network topology was determined by changing the number of hidden neurons (from 1 to 10) and the type of transfer functions. The input variables were temperature (X_1), Sodium hydroxide concentration (X_2), and two-phase volume ratio (X_3), while the output response was the predicted extraction percentage. The experimental data set were divided into two groups, including training and testing data. The experiments produced by CCD (20 data points) were used for training the network and complementary experiments (7 data points) were employed in the range of independent variables as the testing data for model validation.

3. Predictive Ability of ANN and RSM Models for Mercaptan Extraction.

The performance of ANN and RSM models to predict the mercaptan extraction percentage was evaluated by the root mean square error (RMSE), mean relative error (MRE), and determination coefficient (R^2) based on the following equations:

$$RMSE = \sqrt{\frac{1}{N}\sum_{i=1}^{N}(y_i - y_{t,i})^2} \tag{10}$$

$$MRE(\%) = \frac{100}{N}\sum_{i=1}^{N}\frac{|y_{t,i} - y_i|}{y_{t,i}} \tag{11}$$

$$R^2 = 1 - \frac{\sum_{i=1}^{N}(y_i - y_{t,i})^2}{\sum_{i=1}^{N}(y_{t,i} - y_a)^2} \tag{12}$$

where N, y, y_t and y_a are the number of data points, predicted data, actual data, and the average of actual data, respectively.

4. Genetic Algorithm

Genetic algorithm (GA) is one of the random search algorithms which uses genetic evolution as a problem-solving model [38]. GA is commonly used to find the optimal points of mathematical models in various processes. In many optimization problems, the genetic algorithm is used to maximize or minimize the objective function. At first, GA produces an initial value of a random solution population for decision variables. Consequently, four main operators consist of evaluation, selection, crossover, and mutation are performed to produce a new generation [39]. These operations are iterated to develop the solution. When one of the possible termination criteria is observed, the iteration process is stopped. The termination criteria can be observed if an acceptable solution level for the optimization process is attained, or if a certain number of generations without fitness development occurs; or if the maximum number of generations is used. Finally, GA selects the best population of decision variables from the final generation as the required response. In this work, the decision variables are temperature, sodium hydroxide solution, and two-phase volume ratio. Moreover, the predicted equation of the ANN model was considered as the objective function with the aim of maximizing the extraction percentage.

RESULTS AND DISCUSSION

1. RSM Modeling

The design of experiments was performed based on coded levels of the three variables, which resulted in 20 experimental runs with six replicates at the central point. Table 3 shows the experimental and predicted results of CCD.

Based on the experimental results and the coded values of variables, the quadratic regression model for prediction of extraction percentage was demonstrated as the following equation:

$$E = 75.2673 - 2.9863X_1 + 3.2152X_2 + 2.6228X_3 - 0.9124X_2^2 - 0.9033X_3^2 \tag{13}$$

In this regression equation, E, X_1, X_2, and X_3 are the values of the extraction percentage, temperature, sodium hydroxide concentration, and two-phase volume ratio, respectively. Table 4 shows the analysis of variance (ANOVA) results for this study.

The model F-value (159.62) and P-value (<0.0001) show that

Table 3. The central composite design and responses for extraction percentage

Run	X_1	X_2	X_3	Mercaptan extraction percentage	
				Experimental	Predicted
1	308.15	15	0.10	74.93	75.26
2	303.15	15	0.10	81.92	81.24
3	305.65	12.50	0.75	69.98	70.60
4	308.15	15	0.10	73.99	75.26
5	308.15	15	0.10	75.54	75.26
6	308.15	15	0.15	76.96	76.90
7	305.65	17.50	0.125	82.47	82.27
8	308.15	10	0.10	66.06	65.19
9	310.65	12.50	0.125	69.22	69.87
10	310.65	17.50	0.75	70.56	71.05
11	308.15	15	0.10	75.55	75.26
12	308.15	15	0.10	75.54	75.26
13	308.15	15	0.10	75.54	75.26
14	305.65	17.50	0.75	76.89	77.03
15	305.65	12.50	0.125	75.56	75.84
16	310.65	12.50	0.75	63.64	64.63
17	308.15	20	0.10	77.96	78.04
18	308.15	15	0.05	67.14	66.41
19	310.65	17.50	0.125	76.14	76.30
20	313.15	15	0.10	70.70	69.29

the model was statistically significant. The predicted R-squared (0.9461) is in reasonable agreement with the adjusted R-squared (0.9766) and both of them show adequate consistency. The F-value of lack of fit (1.66) confirms that the model is adequate to predict and describe the extraction percentage in terms of effective variables.

2. ANN Modeling

Error analysis of the ANN model for different topologies was evaluated by RSME, in which the lowest value of RMSE determines the best network topology. The RMSE values for different numbers of neurons and transfer functions of the hidden layer are illustrated in Fig. 2. The logsig transfer function with 5 hidden neurons was chosen as the best topology for the ANN model.

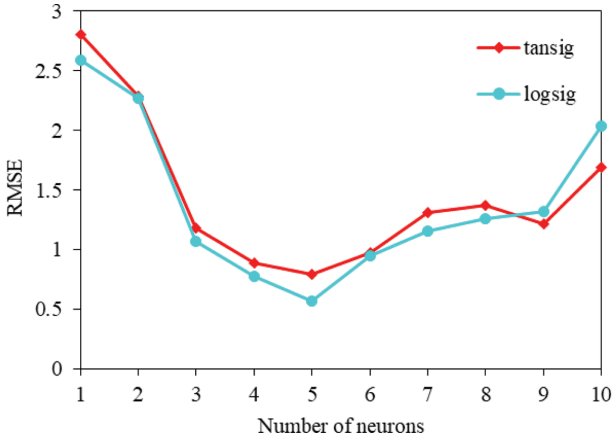

Fig. 2. Values of RMSE for different topologies.

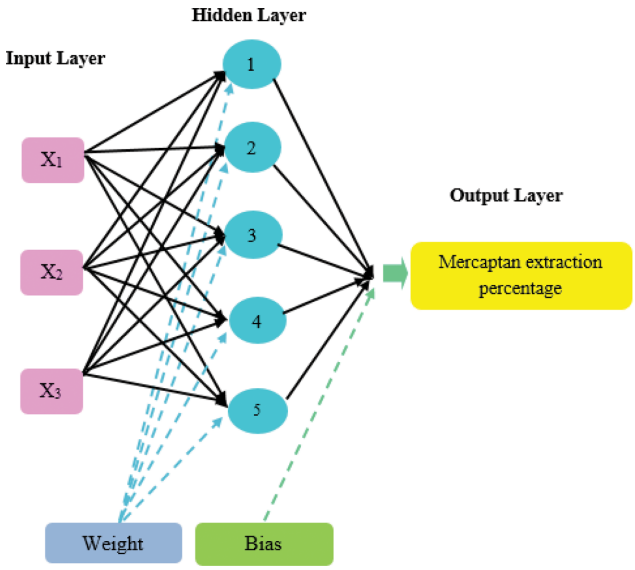

Fig. 3. The topology of the three-layered ANN model (3-5-1) for prediction of the extraction percentage.

Fig. 3 shows the three-layered ANN model (3-5-1) for the modeling study. Moreover, the weights and biases of the best ANN model

Table 4. ANOVA results of the quadratic model for mercaptan extraction

Source	Sum of squares	Df	Mean square	F value	p-Value Prob>F
Model	455.08	5	91.02	159.62	<0.0001
X_1	142.69	1	142.69	250.25	<0.0001
X_2	165.40	1	165.40	290.07	<0.0001
X_3	110.06	1	110.06	193.02	<0.0001
$(X_2)^2$	21.94	1	21.94	38.47	<0.0001
$(X_3)^2$	21.50	1	21.50	37.71	<0.0001
Residual	7.98	14	0.57		
Lack of fit	5.98	9	0.66	1.66	0.2999
Pure error	2.00	5	0.40		
Correlation total	463.06	19			
R-squared=0.9828 (Adj) R-squared=0.9766				(Pred) R-squared=0.9461	

Table 5. Weights and biases of the developed ANN model

Neuron	W_{ji}			b_j	b_z=−0.6574
	X_1	X_2	X_3		W_{zj}
1	3.3795	2.4466	1.3608	−6.0584	−1.0473
2	1.5593	−3.8737	0.8108	−2.6107	−1.0690
3	−1.4125	0.9679	5.9864	2.6569	0.9233
4	−2.7907	−5.5295	1.8113	0.8230	−0.0649
5	−4.5378	1.9907	2.6196	−3.7113	0.7517

are shown in Table 5. Therefore, the mercaptan extraction percentage can be calculated by replacing the weights and biases into Eq. (8).

3. Effect of Independent Parameters on the Mercaptan Extraction

ANOVA results show that there is not any significant interaction parameter in the mercaptan extraction process. Therefore, to analyze the mercaptan extraction process in terms of effective parameters, two parameters were fixed at the zero level and the effect of the third parameter on the extraction percentage was investigated.

3-1. Temperature Effect

As shown in Fig. 4(a), the extraction percentage was considerably decreased with an increase in temperature. Although the mercaptan solubility in alkaline solution does not change significantly with temperature fall, hydrolysis constant is decreased and, consequently, the overall extraction constant is enhanced [2]. However, the lowest temperature for mercaptan extraction from different petroleum products is nearly 293 K, because below this temperature, carbonate and sodium sulfide will precipitate out of the aqueous phase and can block the flow path [32].

3-2. Effect of Sodium Hydroxide Concentration

Experiments were performed at different concentrations of sodium hydroxide to assess the effect of sodium hydroxide concentration on the mercaptan extraction. As is shown in Fig. 4(b), an increase in the sodium hydroxide concentration leads to an enhancement in the extraction percentage. However, the improvement in the mercaptan extraction at the higher sodium hydroxide concentrations is negligible. This is because of the salting-out phenomenon that decreases the partition coefficient of mercaptans [2]. Improving the extraction percentage with an increase in the sodium hydroxide concentration is in agreement with the results obtained by Afshar et al. [9] for LPG demercaptanization.

3-3. Effect of Two-phase Volume Ratio

The sodium hydroxide flow rate was varied from 3.33×10^{-8} to 10×10^{-8} (m^3/s) to 6 mL/min to study the effect of the two-phase volume ratio on the extraction percentage. The LSRN flow rate was kept at 6.66×10^{-7} (m^3/s). As the results demonstrate in Fig. 4(c), with an increase in the volume ratio of sodium hydroxide to LSRN at constant values of temperature and sodium hydroxide concentration, the extraction percentage improves. Indeed, with an increase in the volume ratio of two phases, a higher amount of sodium hydroxide is available in the microchannel that can enhance the driving force of mass transfer between two phases. However, an increase in the volume ratio to more than 0.125 does not have much effect on improving the extraction percentage and only causes more consumption of sodium hydroxide. Akopyan et al. [14] observed similar results for mercaptan extraction from light hydrocarbons with sodium hydroxide and ammonia solution.

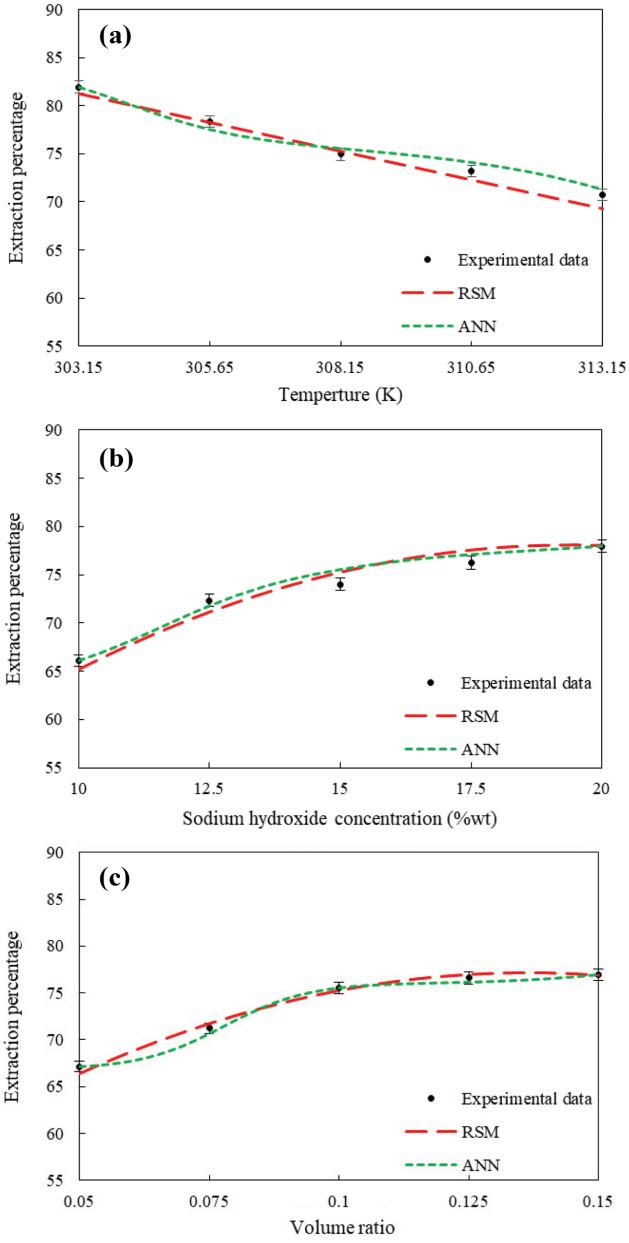

Fig. 4. (a) Effect of temperature on the mercaptan extraction percentage (sodium hydroxide concentration=15 wt%, volume ratio of sodium hydroxide to LSRN=0.10). (b) Effect of sodium hydroxide concentration on the mercaptan extraction percentage (temperature=308.15 K, volume ratio of sodium hydroxide to LSRN=0.10). (c) Effect of volume ratio of sodium hydroxide to LSRN on the mercaptan extraction percentage (temperature=308.15 K, sodium hydroxide concentration=15 wt%).

4. Comparison of the RSM and ANN Models

In this study, to perform a comparison between the validity and precision of RSM and ANN models, the predicted results of these models were evaluated. Figs. 5(a) and 5(b) illustrate the predicted

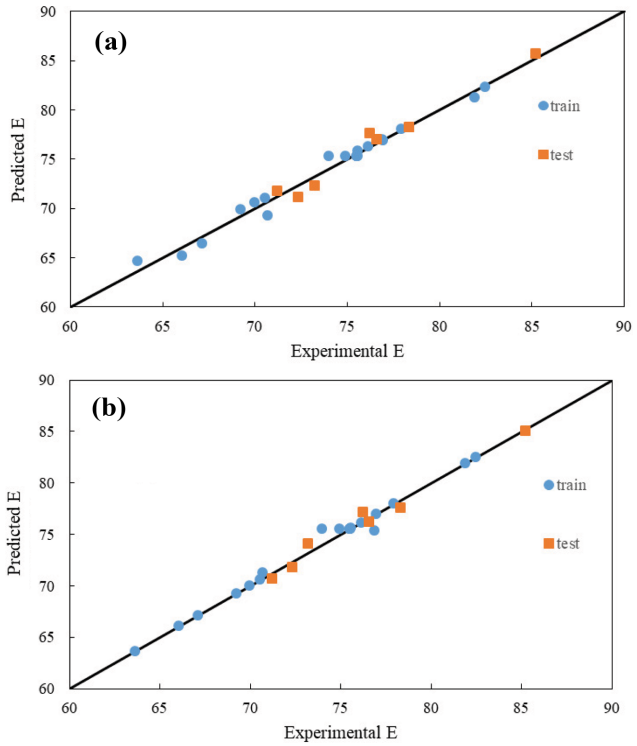

Fig. 5. A comparison between the values of predicted extraction percentage and experimental results for two models. (a) RSM, (b) ANN.

values of RSM and ANN models versus the experimental results. The results represent an excellent agreement between the predicted and experimental values. Besides, the high accuracy of testing data confirms the ANN model validity.

Also, the values of R^2, RMSE, and MRE for the training and testing data are presented in Table 6. As shown, high values of R^2, as well as low values of MRE and RMSE, indicate the high precision of both models. However, the results of this table for the training and testing data indicate that ANN provides a higher R^2 value and lower error values in comparison with the RSM model. Besides, the negligible difference between the testing and training error values in the ANN model affirms the superiority of this model in comparison with the RSM model. The MRE values of the testing data set are 0.9281% and 0.8313% for RSM and ANN models, respectively. These values for MRE of testing data show the higher accuracy of the ANN model in comparison with the RSM model. Therefore, the precision of the ANN prediction is slightly better than that of RSM. Moreover, ANN validity is confirmed by the testing data that were not used in the network training process.

5. Effective Parameters Optimization in the Mercaptan Extraction Process

The comparison between the predicted results of ANN and RSM models showed that the precision of the ANN model is slightly better than that of the RSM model. Therefore, the obtained equation by the neural network was considered as the objective function for the optimization process.

Genetic algorithm was applied to optimize the input parameter values of the developed ANN model with the aim of maximizing the extraction percentage. The optimized values of temperature, sodium hydroxide concentration and two-phase volume ratio were obtained at 303.15 K, 20 wt%, and 0.128, respectively, to achieve the extraction percentage of 85.08%. These results show that the lowest temperature and the highest concentration of sodium hydroxide solution lead to the maximum extraction percentage. Moreover, an increase in the volume ratio of more than 0.128 does not have much effect on improving the extraction percentage and only causes more consumption of sodium hydroxide.

6. Performance Comparison of the Microfluidic System and a Conventional Extractor for the Mercaptan Extraction

To ensure the high performance of the microfluidic system, a comparison was performed between the mercaptan extraction percentage of the microfluidic system and that of a conventional extractor. In this regard, the extraction tower of the LSRN sweetening unit in the Kermanshah oil refinery company (KORC) was considered as the conventional extractor. The flows of LSRN and sodium hydroxide solution in this extraction column are continuous.

The results of LSRN demercaptanization in the extraction column showed that in normal operating conditions (T=308.15 K, NaOH concentration=15 wt%, the volume ratio of sodium hydroxide to LSRN=0.15), mercaptan extraction percentage was in the range of 63-67%. On the other hand, at the same values of operating parameters, the extraction percentage of 77% was obtained by the microfluidic extraction of LSRN. These results reveal the better performance of the microfluidic system for mercaptan extraction compared to the extraction column at the same operating condition. Despite the difference in the scale and capacity of demercaptanization between conventional extractors and microchannels, parallel cascading of the proposed system promises to use it in large scale industrial cases. In fact, the capacity of the microfluidic system can be increased by paralleling microchannels without changing the extraction percentage.

CONCLUSIONS

Mercaptan extraction from LSRN was performed in a T-junction microchannel. One of the major advantages of this research is

Table 6. A comparison between ANN and RSM models for prediction of the extraction percentage

	ANN			RSM		
	Train	Test	Overall	Train	Test	Overall
R^2	0.9881	0.9770	0.9862	0.9828	0.9651	0.9798
RMSE	0.5255	0.6649	0.5650	0.6318	0.8194	0.6854
MRE (%)	0.2951	0.8313	0.4341	0.7071	0.9281	0.7648

to use the high capability of the microfluidic system to improve the extraction of mercaptans. RSM and ANN were applied to investigate the influence of effective parameters on the extraction process and find the optimal operating conditions. The mercaptan extraction process was successfully modeled by these approaches. An appropriate correlation between experimental results and predicted values was observed. The results illustrated that ANN and RSM models are accurate for modeling the mercaptan extraction process. The RMSE, MRE, and R^2 values of the ANN model were 0.5650, 0.4341, and 0.9862, respectively. In comparison, for the RSM model they were 0.6854, 0.7648, and 0.9798. According to the obtained results, the ANN model is more precise compared to the RSM model for predicting the extraction percentage. The influence of independent variables, including temperature, sodium hydroxide concentration, and two-phase volume ratio on mercaptan extraction percentage, was investigated. The independent parameters of the ANN model were optimized by genetic algorithm technique. The maximum extraction percentage of 85.08% was obtained at 303.15 K, sodium hydroxide concentration of 20 wt%, and two-phase volume ratio of 0.128. Furthermore, the results showed that at the same condition of process parameters, the applied microfluidic system has a better performance for the extraction of mercaptans compared with a conventional extractor.

ACKNOWLEDGEMENTS

The authors wish to express thanks to the Kermanshah Oil Refinery Company (KORC) for preparing the LSRN samples.

NOMENCLATURE

b	: bias
COS	: carbonyl sulfide
CS_2	: carbon disulfide
E	: extraction percentage
e	: error term
F	: transfer function
K_E	: overall extraction constant
M	: mercaptan concentration [ppm]
m	: number of input variables
N	: number of data points
n	: number of neurons
R^2	: coefficient of determination
RS^-	: ionized mercaptan
RSH	: mercaptan
W	: weight
X	: independent variables
Y	: predicted response of RSM model
y	: predicted response of ANN model

Subscripts

a	: average
aq	: aqueous phase
H	: hidden layer
in	: inlet
max	: maximum
min	: minimum
norm	: normalized
org	: organic phase
out	: outlet
t	: target data

Abbreviations

ANN	: artificial neural network
ANOVA	: analysis of variance
CCD	: central composite design
GA	: genetic algorithm
KORC	: kermanshah oil refinery company
LPG	: liquefied petroleum gas
LSRN	: light straight-run naphtha
MRE	: mean relative error
RMSE	: root mean square error
RSM	: response surface methodology

REFERENCES

1. M. Khalkhali, A. Ghorbani and B. Bayati, *Polyhedron*, **171**, 403 (2019).
2. D. Yabroff, *Ind. Eng. Chem.*, **32**, 257 (1940).
3. B. Basu, S. Satapathy and A. Bhatnagar, *Catal. Rev. Sci. Eng.*, **35**, 571 (1993).
4. R. Barzamini, C. Falamaki and R. Mahmoudi, *Fuel*, **130**, 46 (2014).
5. Q. Liu, M. Ke, P. Yu, F. Liu, H. Hu and C. Li, *Korean J. Chem. Eng.*, **35**, 137 (2018).
6. M. R. Ehsani, A. R. Safadoost, R. Avazzadeh and A. Barkhordari, *Iran. J. Chem. Chem. Eng.*, **32**, 71 (2013).
7. C. J. LaFoy, US Patent, 4,705,620 (1985).
8. R. Liu, D. Xia, Y. Xiang and Y. Tian, *Pet. Sci. Technol.*, **23**, 711 (2005).
9. A. S. Afshar, S. R. Hashemi, M. Miri and P. Setayeshi, *Pet. Sci. Technol.*, **31**, 2364 (2013).
10. S. Ganguly, N. Rathi and A. Jain, *Pet. Sci. Technol.*, **31**, 1283 (2013).
11. M. Shahrak, E. Ebrahimzadeh and F. Shahraki, *Energy Sources Part A*, **37**, 791 (2015).
12. P. Amani, M. Amani and R. Hasanvandian, *Korean J. Chem. Eng.*, **34**, 1456 (2017).
13. A. Parvareh, *Iran. J. Chem. Eng.*, **14**, 55 (2017).
14. A. Akopyan, B. Andreev, A. Anisimov, E. Eseva, A. Tarakanova, A. Ustinov, A. Kleimenov, D. Kondrashev, D. Khrapov and R. Esipenko, *Russ. J. Appl. Chem.*, **92**, 865 (2019).
15. Y. S. Huh, S. J. Jeon, E. Z. Lee, H. S. Park and W. H. Hong, *Korean J. Chem. Eng.*, **28**, 633 (2011).
16. K.-I. Sotowa, R. Miyoshi, C.-G. Lee, Y. Kang and K. Kusakabe, *Korean J. Chem. Eng.*, **22**, 552 (2005).
17. M. N. Kashid, A. Gupta, A. Renken and L. Kiwi-Minsker, *Chem. Eng. J.*, **158**, 233 (2010).
18. K. K. Singh, A. U. Renjith and K. T. Shenoy, *Chem. Eng. Process.*, **98**, 95 (2015).
19. L. Zhang, F. Xie, S. Li, S. Yin, J. Peng and S. Ju, *Green Process. Synth.*, **4**, 3 (2015).
20. S. Dai, J. Luo, J. Li, X. Zhu, Y. Cao and S. Komarneni, *Ind. Eng. Chem. Res.*, **56**, 12717 (2017).
21. M. Al-Azzawi, F. S. Mjalli, A. Al-Hashmi, T. Al-Wahaibi and B.

Abu-jdayil, *Chem. Eng. Process.*, **140**, 43 (2019).
22. X. Chen, T. Li and Z. Hu, *Microsyst. Technol.*, **23**, 2649 (2017).
23. X. Chen and J. Shen, *Int. J. Heat. Mass. Transfer.*, **106**, 593 (2017).
24. M. Darekar, N. Sen, K. Singh, S. Mukhopadhyay, K. Shenoy and S. Ghosh, *Hydrometallurgy*, **144**, 54 (2014).
25. A. Talebi, T. T. Teng, A. F. Alkarkhi, I. Norli and L. W. Low, *Desalination. Water. Treat.*, **47**, 334 (2012).
26. M. Asadollahzadeh, H. Tavakoli, M. Torab-Mostaedi, G. Hosseini and A. Hemmati, *Talanta*, **123**, 25 (2014).
27. M. Karmakar, M. Mahapatra and N. R. Singha, *Korean J. Chem. Eng.*, **34**, 1416 (2017).
28. S. Yildiz, *Korean J. Chem. Eng.*, **34**, 2423 (2017).
29. B. Kim, Y. Choi, J. Choi, Y. Shin and S. Lee, *Korean J. Chem. Eng.*, **37**, 1 (2020).
30. S. Uslu, *Fuel*, **276**, 117990 (2020).
31. UOP163-10, Hydrogen Sulfide and Mercaptan Sulfur in Liquid Hydrocarbons by Potentiometric Titration, ASTM International, West Conshohocken, PA, 2010, www.astm.org.
32. A. S. Afshar and S. R. Hashemi, *Int. J. Chem. Biomol. Eng.*, **79**, (2011).
33. M. Filiz, N. Sayar and A. Sayar, *Hydrometallurgy*, **81**, 167 (2006).
34. G. R. Daham, A. A. AbdulRazak, A. S. Hamadi and A. A. Mohammed, *Korean J. Chem. Eng.*, **34**, 2435 (2017).
35. A. Fazlali, P. Koranian, R. Beigzadeh and M. Rahimi, *Korean J. Chem. Eng.*, **30**, 1681 (2013).
36. M. Izadi, M. Rahimi and R. Beigzadeh, *Chem. Eng. J.*, **356**, 570 (2019).
37. M. Rahimi, M. Hajialyani, R. Beigzadeh and A. A. Alsairafi, *Chem. Eng. Res. Des.*, **98**, 147 (2015).
38. H. Sahraie, M. R. Mirani, M. H. Ahmadi and M. Ashouri, *Energy Convers. Manage.*, **99**, 81 (2015).
39. M. R. Mirani and F. Rahimpour, *J. Chromatogr. A*, **1422**, 170 (2015).